ELSEVIER

Journal of Alloys and Compounds 404–406 (2005) 732–737

Journal of ALLOYS AND COMPOUNDS

www.elsevier.com/locate/jallcom

# Nanocrystalline alanates—Phase transformations, and catalysts

M. Fichtner*, P. Canton, O. Kircher, A. Léon

*Karlsruhe Research Centre, Institute of Nanotechnology, PO Box 3640, D-76021 Karlsruhe, Germany*

Received 7 September 2004; accepted 2 December 2004
Available online 15 July 2005

**Abstract**

X-ray absorption in combination with powder X-ray diffraction and surface analytical studies were performed in order to investigate the chemical state, local order and spatial distribution of Ti in sodium alanate doped with $TiCl_3$ and small Ti clusters. Kinetic investigations of the different hydrogenation and dehydrogenation steps of doped $NaAlH_4$ indicate a nucleation and growth mechanism as rate limiting step in the transformation of the material. The results support a mechanism where Ti has an accelerating effect on the phase transformation, probably by introducing non-thermal defects into the material.

*Keywords:* Metal hydrides; Hydrogen absorbing materials; Aluminum hydrides; X-ray diffraction

## 1. Introduction

After the first stimulating work of Bogdanovic et al. [1], researchers have investigated reversible hydrogen storage properties of sodium alanates (e.g. [2–5]). A succeeding phenomenological study showed that ball milling of $NaAlH_4$ has a remarkable effect in speeding up the decomposition kinetics of the pure compound [2]. Moreover, improvements were reached when the alanate was mixed with a dopant and subjected to ball milling rather than wet impregnation proposed in [1]. Nanocomposites prepared by ball-milling $NaAlH_4$ with Ti compounds such as $TiCl_3$ or Ti alkoxides as catalyst precursor showed superior hydrogenation and dehydrogenation behavior [4]. The latest improvements have been achieved by using a small Ti cluster as dopant [7,8]. The addition of 5 mol% Ti on the basis of the cluster allows a rehydrogenation to 80% of maximum value within 50 s only at 100 °C and 100 bar hydrogen pressure [9].

While there has been a remarkable progress in the development of dopants, only a few attempts of developing suitable alanate-based H carrier materials with higher reversible hydrogen contents have been reported [6,10,11]. In the meantime, sodium alanate has evolved into a model system for the research community and efforts are being made to finding out more about the details of the transformation mechanism of functional nanocomposites based on $NaAlH_4$ as hydrogen carrier. In particular, possible intermediates in the transformation, the rate-determining reaction steps, and the role of Ti dopants are subject of research.

The present work aims at giving an insight into the fate of Ti precursors during ball milling and dehydrogenation cycling. Moreover, a detailed analysis of XRD patterns and depth profiling of doped alanate sample are performed to obtain information about the spatial distribution of Ti and effects of ball milling. Finally, the relationship between the kinetic measurements made and the state and possible role of Ti in the material will be highlighted.

## 2. Experimental

All sample preparations were done in an argon-filled glove box equipped with a recirculation system to keep the water and oxygen concentrations below 1 ppm. Chemical operations were performed on the bench under a nitrogen atmosphere using Schlenk tube techniques. Ball milling was performed with a Fritsch P6 planetary mill at 600 rpm using

---

* Corresponding author. Tel.: +49 7247 82 5340; fax: +49 7247 82 6368.
*E-mail address:* fichtner@int.fzk.de (M. Fichtner).

0925-8388/$ – see front matter © 2005 Elsevier B.V. All rights reserved.
doi:10.1016/j.jallcom.2004.12.178

silicon nitride balls and a vial with a ball to powder weight ratio of about 20:1. The vial was filled and sealed in the glove box. $TiCl_3$ (Sigma–Aldrich, 99.999% purity) was used as received. Purification of $NaAlH_4$ and the synthesis of Ti clusters are described in detail in Ref. [7]. Experimental details concerning the X-ray absorption and X-ray photoelectron measurements can be found elsewhere [12,19].

For XRD experiments, the powder was prepared and measured under an argon atmosphere in a special XRD sample holder. A Philips X'PERT diffractometer equipped with a focusing graphite monochromator on the diffracted beam and a proportional counter was used. Moreover, a divergence and antiscatter slit of 0.5°, a receiving slit of 0.2 mm, and Ni-filtered Cu Kα radiation (40 mA, 50 kV) were employed. The patterns were recorded at 295 K with a step size of 0.05° in a 10–140° $2\theta$ range using a counting time of 5 s per run. Total counting time per step was 30 s.

Powder samples were prepared for SIMS and SNMS measurements by pressing small amounts of doped alanate powder in In foil (99.999%) and mounting a 1 $cm^2$ piece under a Ta mask (orifice 7 mm) on a sample holder of an INA-3 instrument by SPECS GmbH. The samples were transferred to the instrument under an Ar atmosphere, and the mounted sample holder was cooled with a liquid nitrogen flow for the measurements. SNMS experiments were conducted as described in [17]. Charging the non-conductive samples was avoided by performing the measurements in a high-frequency sputter mode. At target potential time, $Ar^+$ ions are attracted from the Ar plasma in front of the sample to sputter the sample. At zero potential time, plasma electrons are attracted from the plasma to compensate charged sample areas.

## 3. Results

### 3.1. State of the catalyst

The chemical state of Ti in $NaAlH_4$ doped with 5 mol% of either $TiCl_3$ or $Ti_{13} \cdot 6THF$ was investigated using X-ray absorption spectroscopy and X-ray photoelectron spectroscopy.

### 3.1.1. $TiCl_3$ doped samples

XANES [12] and XPS analysis [19] confirm earlier assumptions of a reduction of the precursor $TiCl_3$ occurring during ball milling [4]. The titanium is partially reduced to the metallic state after 2 min of ball milling and completely reduced after 30 min of ball milling. Moreover, Ti remains in a zero-valent state during desorption and absorption of hydrogen. EXAFS analysis [12] suggests a local structure around the Ti atoms consisting only of Ti neighbors after ball milling and during subsequent release and uptake of hydrogen. Furthermore, the structure formed after ball milling is in a distorted state but the local order evolves and tends to a higher order from the ball-milled state to the absorbed one. The coordination environment found from the refinement of the EXAFS function $\chi(k)$ is close to that of metallic titanium. The presence of the beat node at high k-space range as well as the fail of the refinement with Al as backscatterers around the Ti atoms suggests that the formation of an alloy between Ti and Al in the first cycle is not supported. The comparison of those data with references such as TiAl, $Ti_3Al$ or $TiAl_3$ will be published in a forthcoming paper.

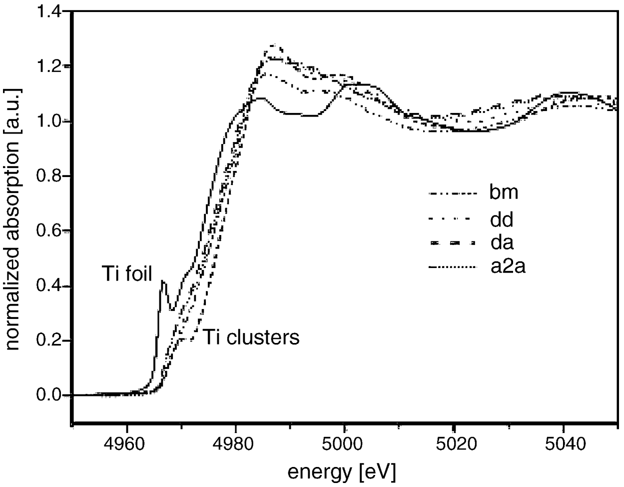

Fig. 1. Normalized Ti K-edge XANES spectra of $NaAlH_4$ doped with 5 mol% of Ti ($Ti_{13} \cdot 6THF$ basis) at different stages. Spectra of pure Ti metal and $Ti_{13} \cdot 6THF$ are shown for comparison.

### 3.1.2. $Ti_{13} \cdot 6THF$ doped samples

The $Ti_{13} \cdot 6THF$ structure consists of a metal core having an icosahedral shape and six THF ligands. The O atom of each THF molecule is bound to three Ti atoms. $Ti_{13} \cdot 6THF$ is a two-shell cluster with a Ti–O distance of 2.02 Å and a Ti–Ti distance of 2.89 Å. Fig. 1 shows the normalized Ti K-edge XANES spectra of sodium alanate doped with Ti clusters after ball milling (bm), at defined stages of the dehydrogenation (dd), hydrogenation (da) and after the second absorption reaction (a2a). For comparison the spectra of the Ti foil and the pure $Ti_{13} \cdot 6THF$ ($Ti_{13}$) is added. From the first derivatives of the spectra (not shown) it can be seen that the first inflection point in spectra ($Ti_{13}$), (bm) and (dd) is at 4967 eV, whereas it is lowered to 4966.5 eV in the spectra (da) and (a2a). This indicates that Ti in the clusters is transformed from the coordinated ('sub-oxide') to the metallic state during the hydrogenation reaction. First EXAFS analysis confirms that in the case of the cluster the local structure around Ti atoms is changing during the hydrogenation reaction. Comparison of the Fourier Transform magnitude of the EXAFS signal shows that the amplitude of the oxygen shell is reduced during the hydrogenation and subsequent cycles. This indicates that the Ti–O bonds are stripped off from the metal core during the first absorption reaction.

### 3.2. Distribution of Ti in doped samples

It was suggested in earlier work that Ti would not only stay at the surface, but might also migrate into the lattice, where it could assist the phase transformation [13]. This presumption was supported by theoretical work which showed that partial replacement of Al by Ti may be beneficial from an energetic point of view [14]. However, no experimental evidence has been presented for the assumption yet.

### 3.2.1. XRD analysis

Our approach was to check first whether indications of a Ti/Al exchange could be found in X-ray diffraction data. In order to investigate possible structural modifications in doped sodium alanate, XRD patterns were taken from purified $NaAlH_4$ which was ball-milled for 30 min either with 5 mol% of $TiCl_3$ or with of 5 mol% $Ti_{13} \cdot 6THF$.

$NaAlH_4$ crystallizes in the tetragonal space group $I4_1/a$, $Z = 4$, $a = 0.5025$ nm, $c = 1.136$ nm, Na in 4a (0, 1/4, 1/8), Al in 4b (0, 1/4, 5/8), H in 16f (x, y, z). The H general position and the thermal parameters for Al, Na and H were taken from neutron diffraction data [16]. $Na_3AlH_6$ crystallizes in the monoclinic space group $P2_1/n$. Al is cubic, space group $Fm3m$, $a = 0.4049$ nm. The XRD data were analyzed by Rietveld refinement using the DBWS-9600 code written by Sakthivel and Young [15].

*3.2.1.1. Ti cluster doped samples.* The pattern contained contributions coming from $NaAlH_4$ phase, traces of the first stage decomposition of the alanate $Na_3AlH_6$ and some metallic aluminum. There were no indications of any preferred orientation in the samples.

The results of the Rietveld refinement are reported in Fig. 2. The inset is the enlargement of the $2\theta$ range from 17 to 22° showing the (0 1 1) reflection of the $NaAlH_4$ phase.

It is clearly evident from both figures that some of the alanate intensities are not properly described by the refinement. The attempt of refining the thermal parameters did not improve the intensities description. A refinement of the Al occupation number (with the other occupation numbers and all the thermal parameters kept fixed) showed that Al electron density is not sufficient to describe properly some of the Bragg reflections. In contrast to this, the refinement of the Na occupation number revealed a full occupation of the site and no change in the reflection description.

For these reasons, a Ti cation (up to 20 at.%) was randomly substituted for Al to see whether the intensities description improved. The total amount of Al + Ti was equal to the crystallographic site occupation number. The two Rietveld calculated patterns with and without Ti at the Al position inside the lattice are compared in Fig. 3.

Even if the starting amount of Al and Ti corresponded to a fully occupied site, the results obtained by the refinement could indicate the presence of vacancies in the alanate structure. Both Ti and Al can be present but the global amount is lower than the stoichiometric value. However, due to the high correlations between thermal parameters and occupation numbers further investigations are in progress to determine if Ti substitutes for Al and the exact amount of Ti, if present, inside the lattice.

*3.2.1.2. $TiCl_3$ doped samples.* The XRD pattern was found to be composed of the $NaAlH_4$ phase, metallic Al, and some traces of $TiCl_3$. $Na_3AlH_6$ was not present. As for the sample ball-milled with Ti clusters the $NaAlH_4$ intensities were not properly described using a pure sodium alanate phase. The same refinement procedure used for the Ti cluster sample and described in the preceding paragraph was applied here.

Also in this case, the results of the refinement showed that the Al site could accommodate Ti atoms. Again, a high correlation between thermal parameters and occupation numbers was observed; the refinement of the thermal parameters with the occupation numbers for the $NaAlH_4$ phase without any Ti inside being kept fixed did not result in any improvement of the XRD data description. Only a low amount of vacancies was found inside the lattice. This could probably be due to the small quantity of Ti present in the lattice.

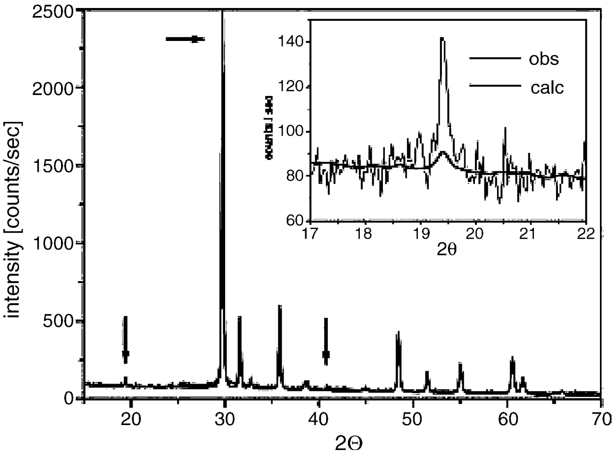

Fig. 2. Observed and calculated pattern of $NaAlH_4$ doped with 2 mol% Ti on Ti cluster basis. The arrows indicate major deviations between the observed and calculated data.

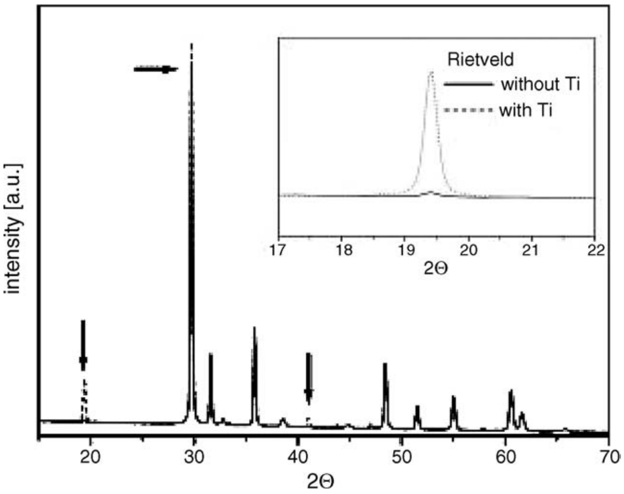

Fig. 3. Rietveld calculated pattern with Ti partly substituting Al and without Ti in the lattice. The arrows indicate major deviations between the two simulated patterns.

### *3.2.2. Surface analysis*

To investigate the spatial distribution of Ti in Ti doped sodium alanate samples, surface analytical studies have been performed. Secondary ion mass spectrometry (SIMS) was used to determine chemical species at the outer surface of doped alanate samples. Secondary neutral mass spectrometry (SNMS) was applied for depth-profiling. SNMS is a surface analysis method which detects secondary neutrals emitted from a sputtered surface and allows for the semi-quantitative determination of atom concentrations also of non-conducting powder materials with nanometer-resolution [17]. The yield of sputtered secondary ions strongly depend on the ionization probability at the actual surface. Therefore, SIMS cannot be used to quantify species with a varying surface composition. However, it gives information on the elemental composition, and, as sputtered cluster ions carry information about neighboring atoms on a samples surface, the method can be used for chemical speciation of complex salts [18].

*3.2.2.1. SIMS measurements.* SIMS spectra of positive secondary ions were taken from a fresh sample which was prepared by ball milling of $NaAlH_4$ with 4 mol% $TiCl_3$ for 300 min. Fig. 4 shows the mass spectrum with the most intense signals of $Na^+$ ($m/z = 23$) and $Al^+$ ($m/z = 27$) coming from the alanate. $K^+$ ($m/z = 39, 41$) is a typical trace found in sodium containing salts, $In^+$ ($m/z = 115, 113$) was emitted from the embedding In foil. Surprisingly, the Ti signal ($Ti^+$ ($m/z = 46, 47, 48$) is comparably low at the surface of the composite particles. The spectrum rather shows intense cluster signals coming from $Na_2^+$ ($m/z = 46$, normally observed with high $Na^+$ intensities) and $Na_2O^+$ ($m/z = 62$). The $NaAl^+$ ($m/z = 50$), $NaAlO^+$ ($m/z = 66$) and $Na_2AlO^+$ ($m/z = 89$) signals suggest Na and Al in close vicinity, which is probably due to an alanate species. The oxygen in the cluster ions indicates a partly oxidized alanate species at the surface, due to a strong interaction of ball-milled alanate even with traces of oxygen. Moreover, the strong signal of the $Na_2Cl^+$ cluster ion is a direct proof of the precursor $TiCl_3$ having reacted with sodium alanate to form NaCl.

*3.2.2.2. SNMS measurements.* It was not possible to determine the depth propagation and resolution of alanate samples as standards are lacking. However, a rough estimation is possible by comparison with data obtained with a layer pigment (Iriodin 9444, MERCK). The pigment particles consist of a mica core coated with a 170 nm $TiO_2$ layer followed by a 35 nm $Cr_2O_3$ layer.

It took 1000–1100 s to sputter through the $Cr_2O_3$ layer which corresponds to a depth propagation of 0.03–0.035 nm/s. In the second layer, the depth propagation was 0.04–0.045 nm/s. The time difference between the 33% and the 67% intensity value of the increasing Ti signal after sputtering the first layer was taken to calculate the depth resolution which was 8–9 nm in this particular sample.

Doped alanate samples were prepared by ball-milling $NaAlH_4$ with 4 mol% $TiCl_3$ for 3, 30, and 300 min. Intensities of Na ($m/z = 23$), Al ($m/z = 27$), Cl ($m/z = 350$), Ti ($m/z = 48$), and In ($m/z = 115$) were recorded as a function of time. Fig. 5 shows the Ti intensities for the three differently milled samples as well as for a sample prepared by mixing ball-milled alanate with 4 mol% $TiCl_3$ in an agate mortar. The data exhibits a development of the Ti intensity with depth, depending on the milling time. The sample which was ball-milled for 3 min showed a maximum of the Ti concentration in the outer region. The data suggests that a Ti rich layer forms at the outer surface of the alanate particles during short-term ball-milling. From the depth propagation values mentioned above, the thickness of this layer can be estimated to be some 30–40 nm. The data also show that the layer vanishes and Ti is dispersed in the material when the sample is ball-milled for 30 min or more.

Obviously, the Ti concentration is reduced at the outer surface of samples that have been ball-milled for 30 and 300 min, which is accordance with the SIMS data presented

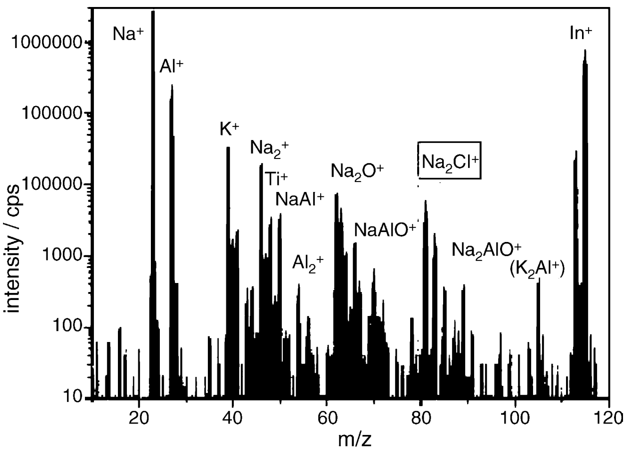

Fig. 4. SIMS spectrum of the outer surface of sodium alanate doped with 4 mol% $TiCl_3$ and ball-milled for 300 min.

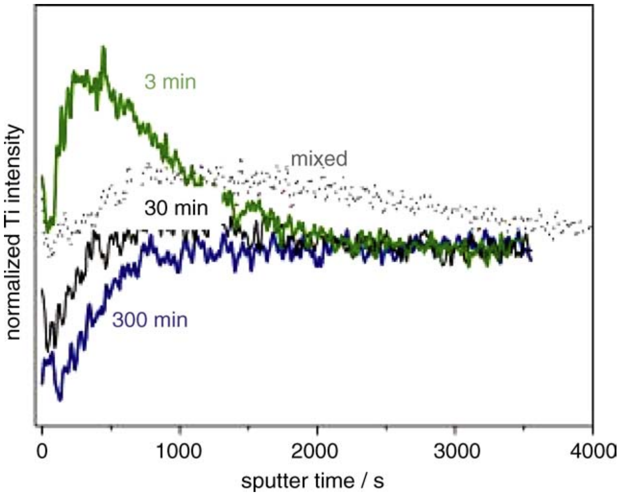

Fig. 5. SNMS time profile of sodium alanate doped with 4 mol% $TiCl_3$ and ball-milled for 3, 30, and 300 min or loosely mixed. The shown Ti intensities were normalized for comparison.

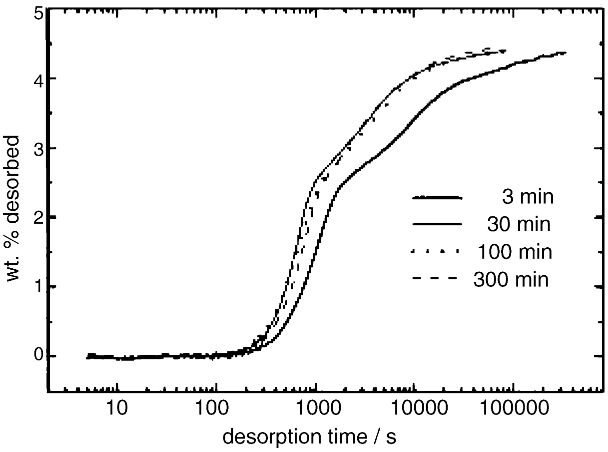

Fig. 6. Isothermal decomposition of $NaAlH_4 + 2$ mol% $TiCl_3$ at 150 °C, in the third desorption–absorption cycle (experimental details described in [7]).

above. This is also confirmed by XPS measurements of doped sodium alanate, where a reduced Ti concentration was found at the surface of samples that had been subjected to longer ball milling [19]. The findings support the assumption that Ti is driven into the material by high energy ball milling.

### *3.3. Phase transformations*

Phase separation is observed when the alanate is thermally decomposed into $Na_3AlH_6$ and Al or NaH and Al, depending on the stage of decomposition [1,13]. Taking low concentrations of the Ti cluster as dopant, kinetic studies showed that nucleation and growth of the forming phases are rate limiting for the transformations during hydrogen exchange for the observed temperature range of 100– 150 °C [20]. The study indicates that diffusion of the involved species (NaH + Al and $Na_3AlH_6$ + Al) limits the alanate formation rate during the rehydrogenation of the decomposed material [20].

Fig. 6 shows the kinetic data for the decomposition of doped $NaAlH_4$ which was ball-milled for various times. It is evident that samples ball-milled for 3 min exhibit the lowest transformation rates, whereas all other samples transform considerably faster with about the same rates. The corresponding absorption kinetics are not shown here, but exhibit the same behavior.

## 4. Discussion

The Ti catalyst has a large influence on the rate of H release and uptake and the role played by Ti in the materials transformations is of great importance. It is expected that a Ti containing phase may act as chemisorption site for the molecular hydrogen, which was also demonstrated in isotope scrambling experiments [21].

However, the rate limiting step observed is governed by nucleation and growth as was shown in kinetic studies. The formation rate of the alanate phase during the rehydrogenation was found to be limited by diffusion of two solid phases, which have to react with each other under the presence of hydrogen.

Hence, we assume that Ti has an influence also on the rate of these processes. The results presented in Section 3.2 indicate that Ti atoms may be driven into the material by ball milling for 30 min or longer. Moreover, the fact that Ti is dispersed in the material correlates with the rate of hydrogen exchange, which corresponds to the rate of phase transformation. If chemisorption at a Ti containing phase in the surface controlled the rate of transformation, the reduced Ti concentration at the outer surface in case of longer milling times would favor a contradictory trend of the data. It is therefore unlikely that the Ti concentration at the outer surface has a dominating influence on the catalytic effect.

The XRD study in Section 3.2 suggests that a part of the Ti can also substitute Al in the alanate lattice. There, it can create non-thermal defects due to its different size, depending on the valence state, and coordination behavior when compared to Al. Defects are known to enhance diffusion extraordinarily and hence play a determining role for materials transport in many solids. From the findings mentioned above, we assume that Ti substituting Al in the alanate lattice is at least partly responsible for the enhanced transformation rates. The presumption is supported by the observation that Ti clusters create more vacancies in the alanate than $TiCl_3$. This could explain the higher transformation rates of Ti cluster-doped samples.

Moreover, if the whole transformation process is considered a consecutive reaction of a fast chemisorption step and a rate-determining, defect-enhanced transformation in the solid, it becomes clear why other dopants with much better chemisorption properties hardly have any catalytic effect. Although they may increase the rate of the chemisorption step, the rate of the second, rate-determining step, is low because of the lack of defects created by the substitution of Al in the lattice.

## 5. Summary

The chemical state and spatial distribution of Ti in doped sodium alanate samples was investigated by a combination of X-ray absorption (XANES, EXAFS), X-ray diffraction (XRPD) and surface analytical (SIMS, SNMS, XPS [19]) methods.

XANES and EXAFS data indicates that $TiCl_3$ is reduced to $Ti^0$ during the ball-milling process and stays in this state during desorption and absorption of hydrogen. The next neighbors of Ti in freshly ball-milled, in partially dehydrogenated and in partially rehydrogenated samples were determined to be at typical Ti–Ti distances and no hint for the formation of an alloy with Al could be found at this early stage of the process. X-ray diffraction data and Rietveld refinement on $NaAlH_4$ samples doped with Ti clusters and $TiCl_3$ suggest the incorporation of Ti into the alanate lattice where it can stay at Al sites. The data also indicate the formation of vacancies in the material.

XPS and SNMS data of $TiCl_3$ doped samples exhibit an initially formed Ti rich layer at the surface which is distributed in the material when the material is ball-milled for 30 min or longer. The remaining surface region appears to be depleted of Ti, which is distributed in the remaining material, according to SNMS and XPS data.

The experimental observations and correlations support a mechanism where the number of defects created by a partial substitution of Al by Ti determines the rates of transformation of the alanate material.

## References

[1] (a) B. Bogdanovic, M. Schwickardi, J. Alloys Compd. 253–254 (1997) 1.
(b) B. Bogdanovic, R.A. Brand, A. Marjanovic, M. Schwickardi, J. Tölle, J. Alloys Compd. 302 (2000) 36.

[2] A. Zaluska, L. Zaluski, J.O. Ström-Olsen, J. Alloys Compd. 298 (2000) 125.

[3] C.M. Jensen, K.J. Gross, Appl. Phys. A 72 (2) (2001) 213.

[4] K.J. Gross, G. Sandrock, G.J. Thomas, J. Alloys Compd. 330–332 (2002) 691.

[5] R.A. Zidan, S. Takara, A.G. Hee, C.M. Jensen, J. Alloys Compd. 285 (1999) 119.

[6] J. Chen, N. Kuriyama, Q. Xu, H.T. Takeshita, T. Sakai, J. Phys. Chem. B 105 (2001) 11214.

[7] M. Fichtner, O. Fuhr, O. Kircher, J. Rothe, Nanotechnology 14 (2003) 778.

[8] B. Bogdanovic, M. Felderhoff, S. Kaskel, A. Pommerin, K. Schlichte, F. Schüth, Adv. Mater. 15 (2003) 1012.

[9] M. Fichtner, O. Fuhr, O. Huebner, O. Kircher, W. Klopper, A. Léon, Proceedings of the Seventh International Conference on Nanostructured Materials, NANO 2004, Wiesbaden, Germany, June 20–24, 2002.

[10] K. Hosokawa, Thesis, Iowa State University, Ames, IA, 2002.

[11] M. Fichtner, O. Fuhr, J. Alloys Compd. 345 (2002) 286.

[12] A. Léon, O. Kircher, J. Rothe, M. Fichtner, J. Phys. Chem. B 108 (2004) 16372.

[13] K.J. Gross, S. Guthrie, S. Takara, G. Thomas, J. Alloys Compd. 297 (2000) 270.

[14] O.M. Løvvik, S.M. Opalka, Phys. Rev. B 71 (2005) 54103.

[15] A. Sakhtivel, R.A. Young, User's Guide to Programs DBWS-9OO6PC, Georgia Institute of Technology, Atlanta, GA, USA, 1990.

[16] B.C. Hauback, H.W. Brinks, C.M. Jensen, K. Murphy, A.J. Maeland, J. Alloys Compd. 358 (2003) 142.

[17] J. Goschnick, C. Natzeck, M. Sommer, Appl. Surf. Sci. 144–145 (1999) 31.

[18] M. Fichtner, J. Goschnick, H.J. Ache, Fresenius J. Anal. Chem. 348 (1994) 201.

[19] A. Léon, D. Schild, M. Fichtner, J. Alloys Compd., this issue.

[20] O. Kircher, M. Fichtner, J. Appl. Phys. 95 (13) (2004) 7748.

[21] F. Schüth, B. Bogdanovic, M. Felderhoff, Chem. Commun. 20 (2004) 2249.